

Effect of Strontium substitution on the structural and magnetic properties of $\text{La}_{1.8}\text{Sr}_{0.2}\text{MMnO}_6$ (M = Ni, Co) layered manganites

Syeda Karimunnesa^{a, b}, Bashir Ahmmad^c and M. A. Basith^{a*}

^aDepartment of Physics, Bangladesh University of Engineering and Technology, Dhaka, Bangladesh

^bDepartment of Physics, Chittagong University of Engineering and Technology, Chittagong, Bangladesh

^cGraduate School of Science and Engineering, Yamagata University, 4-3-16 Jonan, Yonezawa 992-8510, Japan

Abstract

Sr substituted perovskites $\text{La}_{1.8}\text{Sr}_{0.2}\text{MMnO}_6$ (M = Ni, Co) were synthesized using solid state reaction technique to present a systematic study on their morphological, structural and magnetic properties. The average grain size of the as-prepared $\text{La}_{1.8}\text{Sr}_{0.2}\text{NiMnO}_6$ samples are in the range of 0.2~0.7 μm and those for $\text{La}_{1.8}\text{Sr}_{0.2}\text{CoMnO}_6$ manganites are 0.1~2.8 μm , which is significantly less than that of unsubstituted $\text{La}_2\text{NiMnO}_6$ (LNMO) and $\text{La}_2\text{CoMnO}_6$ (LCMO) manganites. The XPS analysis enlightened about phase purity, binding energy and oxygen vacancy of $\text{La}_{1.8}\text{Sr}_{0.2}\text{MMnO}_6$ manganites. The Sr substituted LNMO has revealed a sharp ferromagnetic to paramagnetic phase transition at 160 ± 2 K which is about 120 K less than that of parent LNMO. The Sr substituted LCMO exhibited such a transition at 220 ± 2 K which is 8 K less than that of parent LCMO. The temperature dependent magnetization measurements suggest that the effect of Sr on the transition temperature in LNMO is more significant than that of LCMO.

Keywords: Layered manganites; XPS analysis; magnetization; magnetic transition.

Introduction

Perovskite manganites exhibit a wide range of functional properties, such as colossal magneto-resistance, magnetocaloric effect, multiferroic property and some interesting physical phenomena including spin, charge and orbital ordering. The double perovskites La_2MMnO_6 (M = Ni, Co) are reported to exhibit ferromagnetic behavior and a magnetodielectric effect near room temperature [1-6], making them a promising material for the next-generation memory devices. A relatively high ferromagnetic Curie temperature (T_C) is found to be strongly dependent on the M^{2+} and Mn^{4+} cations ordering, as well as on the M-O-Mn superexchange interaction.[4, 7] The perovskite manganites classes of materials $\text{La}_2\text{NiMnO}_6$ (LNMO) and $\text{La}_2\text{CoMnO}_6$ (LCMO) have attracted considerable interest in recent years due to their rich physics [8-12] and potential applications [13, 14] in spintronic devices. [15-17] The initial studies on perovskite manganites system were mainly focused on LaMnO_3 which is an antiferromagnetic insulator. [18] It was reported that substitution of La by divalent cations like Sr, Ca and Ba in LaMnO_3 [18, 19] introduces mixed valence on Mn ions and initiate the conventional double-exchange (DE) mechanism. [20, 21] Doping the insulating LaMnO_3 material, in which only Mn^{3+} exists, with the divalent ions (Ca, Ba, Sr, etc.) causes the conversion of a proportional number of Mn^{3+} to Mn^{4+} . The presence of Mn^{4+} , due to the doping, enables the itinerant (e_g) electron of a Mn^{3+} ion to hop to the neighboring Mn^{4+} ion via DE,

Contact: M. A. Basith ✉ mabasith@phy.buet.ac.bd

which mediates ferromagnetism and conduction. However the substitution of La by other divalent cations in perovskite manganites LNMO and LCMO are comparatively less explored. Therefore, in the present investigation, we intend to explore the effect of Sr substitution in LNMO and LCMO manganites systems. Here we have prepared and studied the effects of Sr addition on the structural, morphological and magnetic properties of $\text{La}_{1.8}\text{Sr}_{0.2}\text{MMnO}_6$ manganites synthesized by conventional solid state reaction technique.

Experiment details

The polycrystalline samples having compositions $\text{La}_{1.8}\text{Sr}_{0.2}\text{MMnO}_6$ ($M = \text{Ni, Co}$) were synthesized by using standard solid state reaction technique, as described in detail in our previous investigation. [22] High purity oxides of La_2O_3 (99.9%), SrCO_3 (99.9%), NiO (99.9%), Co_3O_4 (99.9%) and MnCO_3 (99.9%) powders of Sigma-Aldrich, UK, were used as raw materials. The reagents were carefully weighed in proper stoichiometric proportion and mixed thoroughly with acetone. Then it was grounded in an agate mortar for 6 h until a homogeneous mixture was formed. The compacted mixtures of reagents taken in desired cation ratios were calcined at 1100 °C for 12 h in a programmable furnace. The calcined powders were grounded for 6 h by an agate mortar and pestle to get a homogeneous mixture. After the calcinations, 10 mm diameter and 1 mm thick pellets were prepared under a pressure of 12000 P.S.I and finally the samples were sintered at 1300 and 1400 °C for 6 h in air with heating rate 3°C/min for investigations.

The crystal structure of the samples was determined from X-ray diffraction (XRD) data. The XRD patterns were collected at room temperature using a diffractometer (Rigaku Ultimate VII) with CuK_α ($\lambda = 1.5418 \text{ \AA}$) radiation. The microstructure of the surface of the pellets was observed by a field emission scanning electron microscope (FESEM, JEOL, JSM 5800) equipped with the energy dispersive X-ray spectroscopy (EDX). The EDX analysis has been used to determine the overall chemical homogeneity and composition of the samples. X-ray photoelectron spectroscopy (XPS, ULVAC-PHI Inc., 1600) analysis was carried out with a Mg-K_α radiation source. The temperature and field dependent magnetization measurements were carried out both at zero field cooling (ZFC) and field cooling (FC) processes [23] using a Superconducting Quantum Interference Device (SQUID) Magnetometer (Quantum Design MPMS-XL7, USA).

Results and discussions

The XRD patterns of $\text{La}_{1.8}\text{Sr}_{0.2}\text{MMnO}_6$ ($M = \text{Ni, Co}$) are presented in Figure 1. It is observed that all the samples show good crystallization with well-defined diffraction line. All the peaks are indexed in the figure and these peaks are typical for the single phase rhombohedral structure. It was also observed that the positions of the peaks comply with the reported values in $\text{La}_{1.8}\text{Sr}_{0.2}\text{NiMnO}_6$ [24, 25] and $\text{La}_{1.8}\text{Sr}_{0.2}\text{CoMnO}_6$ manganites. [26] Earlier, the unsubstituted polycrystalline La_2MMnO_6 ($M = \text{Ni, Co}$) sample has revealed a monoclinic structure. [26, 27-28] The lattice parameters calculated from the patterns are displayed in Table 1. From the Table 1, it is seen that lattice parameters of 'a' and 'b' in La_2MMnO_6 ($M = \text{Ni, Co}$) and $\text{La}_{1.8}\text{Sr}_{0.2}\text{MMnO}_6$

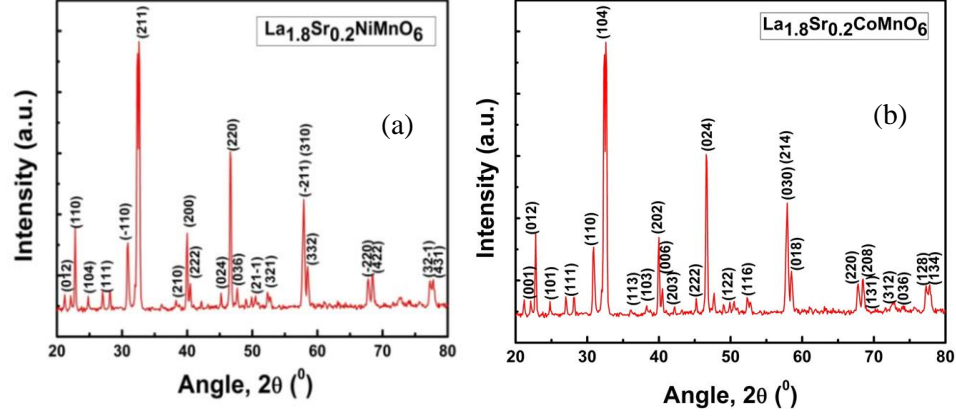


Figure 1. X-ray diffraction patterns at room temperature for $\text{La}_{1.8}\text{Sr}_{0.2}\text{MMnO}_6$ ($\text{M} = \text{Ni}, \text{Co}$). The peaks for all the samples can be well indexed by a simple phase with rhombohedral structure.

($\text{M} = \text{Ni}, \text{Co}$) manganites are almost same, but lattice parameter ‘c’ is changed due to the 10% Sr substitution in La sites of $\text{La}_{1.8}\text{Sr}_{0.2}\text{MMnO}_6$ ($\text{M} = \text{Ni}, \text{Co}$) manganites.

Table 1: Lattice parameters of parent La_2MMnO_6 ($\text{M} = \text{Ni}, \text{Co}$) and $\text{La}_{1.8}\text{Sr}_{0.2}\text{MMnO}_6$ ($\text{M} = \text{Ni}, \text{Co}$) manganites.

Parameters	$\text{La}_2\text{NiMnO}_6$ manganites (Å) [27, 28]	$\text{La}_{1.8}\text{Sr}_{0.2}\text{NiMnO}_6$ manganites (Å) [25, 29]	$\text{La}_2\text{CoMnO}_6$ manganites (Å) [26, 28, 30-31]	$\text{La}_{1.8}\text{Sr}_{0.2}\text{CoMnO}_6$ manganites (Å) [26]
A	5.514	5.515	5.525	5.490
B	5.460	5.515	5.487	5.490
C	7.750	13.620	7.778	13.254

The Figure 2(a) shows the FESEM micrographs of the surface of bulk polycrystalline $\text{La}_{1.8}\text{Sr}_{0.2}\text{NiMnO}_6$ manganites sintered at 1300 °C. It is observed that the surface is non-homogeneous and the grains are agglomerated to some extent. Whereas, with the higher sintering temperature at 1400 °C, the sample became homogeneous and the grains were clearly visible (Figure 2(b)). The FESEM images of $\text{La}_{1.8}\text{Sr}_{0.2}\text{CoMnO}_6$ manganites sintered at 1300 °C (Figure 2(c)) reveal that particles are in good shape and grains are clear. However, for the same sample sintered at 1400 °C (Figure (d)), it is found that the homogeneity of the grains is destroyed. So, the optimum sintering temperatures are considered as 1400 °C and 1300 °C for $\text{La}_{1.8}\text{Sr}_{0.2}\text{NiMnO}_6$ and $\text{La}_{1.8}\text{Sr}_{0.2}\text{CoMnO}_6$ manganites, respectively. Figure 2(b) shows the histogram for average grain size (D) of $\text{La}_{1.8}\text{Sr}_{0.2}\text{NiMnO}_6$ manganite which is calculated by using ImageJ software from the FESEM micrographs and the D values are estimated to around 0.2~0.7 μm from the histogram. Notably, in the parent polycrystalline sample LNMO prepared by the solid state reaction method and sintered at 1400 °C, the average grain size estimated by FESEM image was 2 μm . [27] The histogram for grain size distribution of $\text{La}_{1.8}\text{Sr}_{0.2}\text{CoMnO}_6$ manganites which is worked out from the FESEM image (Figure 2(c)) and the average grain size is estimated at around 0.1~2.8 μm from the histogram. Noticeably, in the original polycrystalline sample

LCMO (sintered at 1300 °C) prepared by the same method, the average grain size was estimated to around 3-5 μm from FESEM image. [26]

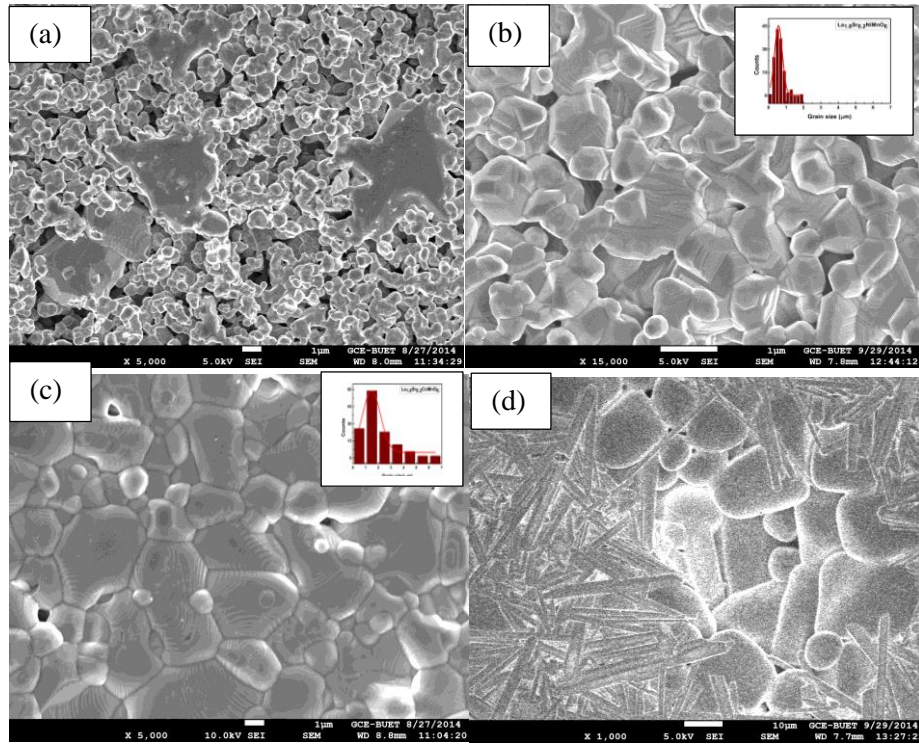


Figure 2. FESEM micrograph of $\text{La}_{1.8}\text{Sr}_{0.2}\text{MMnO}_6$ ($\text{M} = \text{Ni}, \text{Co}$) sintered at 1300 °C (a); (c) and 1400 °C (b); (d). The insets are the corresponding particle size histograms (b) and (c).

From the FESEM (Figure 2) micrographs, it is seen that the average grain size of parent La_2MMnO_6 ($\text{M} = \text{Ni}, \text{Co}$) manganites is greater than that of 10% Sr substitution in La sites of $\text{La}_{1.8}\text{Sr}_{0.2}\text{MMnO}_6$ ($\text{M} = \text{Ni}, \text{Co}$) manganites. The reduced grain size might be associated with different size of ionic radii caused the strain or stress field that hinders the grain growth process. It is clearly seen that the desired elements La, Sr, Ni, Mn and O of $\text{La}_{1.8}\text{Sr}_{0.2}\text{NiMnO}_6$ manganites (Figure 3(a)) and the desired elements La, Sr, Co, Mn and O of $\text{La}_{1.8}\text{Sr}_{0.2}\text{CoMnO}_6$ manganites (Figure 3(b)) are present.

Figures 4(a, b) show the XPS spectra of all elements of bulk $\text{La}_{1.8}\text{Sr}_{0.2}\text{MMnO}_6$ ($\text{M} = \text{Ni}, \text{Co}$) manganites. The photoemission data for all the samples was collected around the Mn 2p doublet, the La 4d and 3d doublet, the O 1s, Sr 3d, Co 2p, Ni 2p and C 1s lines. The XPS technique is a promising tool and is utilized to confirm the oxidation states of Mn, therefore, Mn states were explored elaborately and presented in Figures 4(c, d). Using high-resolution XPS, the two Mn 2p peaks at 642.54 and 654.26 eV, with an energy gap of 11.72 eV, can be assigned to Mn 2p_{3/2} and Mn 2p_{1/2}, respectively as shown in Figure 4(c) for $\text{La}_{1.8}\text{Sr}_{0.2}\text{NiMnO}_6$ manganites. Similarly, the two Mn 2p peaks at 641.32 and 653.05 eV, with an energy gap of 11.73 eV, can be assigned to Mn 2p_{3/2} and Mn 2p_{1/2}, respectively (Figure 4(d)) of $\text{La}_{1.8}\text{Sr}_{0.2}\text{CoMnO}_6$ manganites. However, it

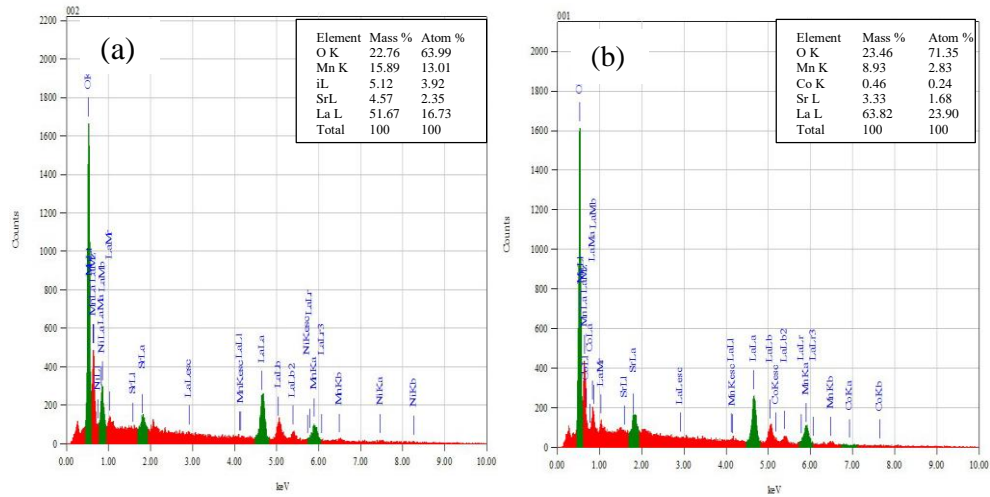


Figure 3. EDX spectrum of $\text{La}_{1.8}\text{Sr}_{0.2}\text{MMnO}_6$ (M = Ni, Co). The insets are the corresponding percentage of mass and atom of the sample.

is difficult to form a definite conclusion about the oxidation state of manganese from Mn 2p spectra, as all manganese oxidation states show the same pattern. Panda et al. [32], reported that the two Mn 2p peaks at 642.40 and 654.13 eV, with an energy gap of 11.73 eV, can be assigned to Mn 2p_{3/2} and Mn 2p_{1/2}, respectively and Kang et al. [33], have reported that all the spectra display the spin-orbit split 2p_{3/2} and 2p_{1/2} peaks located around 642 and 654 eV, respectively which matches well with our reported present results. The Figure 4(e) illustrates the O 1s spectra of bulk $\text{La}_{1.8}\text{Sr}_{0.2}\text{NiMnO}_6$ manganites, which can be fitted to a symmetric Gaussian curve with peak positions 530.28 eV. On the contrary, in Figure 4(f), the O 1s spectra of bulk $\text{La}_{1.8}\text{Sr}_{0.2}\text{CoMnO}_6$ manganites show a slightly asymmetric peak very close to 528.10 eV with additional peak. The asymmetric curves of the bulk sample can be Gaussian fitted by two symmetrical peaks at 528.10 and 531.45 eV, respectively. The lower binding energy peak at 528.10 eV corresponds to the O 1s core spectrum, while higher binding energy peak is attributed to the oxygen vacancies, i.e., to the oxygen related defects [34-38] in the sample. In earlier investigations, a two-peak structure is observed with a component attributed to lattice oxygen at lower binding energies, and a component attributed to surface-or defect related oxygen at higher binding energies. [39-42] This interpretation is more consistent with the observations of the present work.

In the case of bulk $\text{La}_{1.8}\text{Sr}_{0.2}\text{NiMnO}_6$ manganites, temperature dependent zero field cooled and field cooled magnetization curves exhibit a sharp ferromagnetic (FM) to paramagnetic (PM) transition at 160 ± 2 K under the application of a magnetic field of 500 Oe (Figures. 5(a, b)). But for the parent compound LNMO prepared by the same method, it is reported that temperature

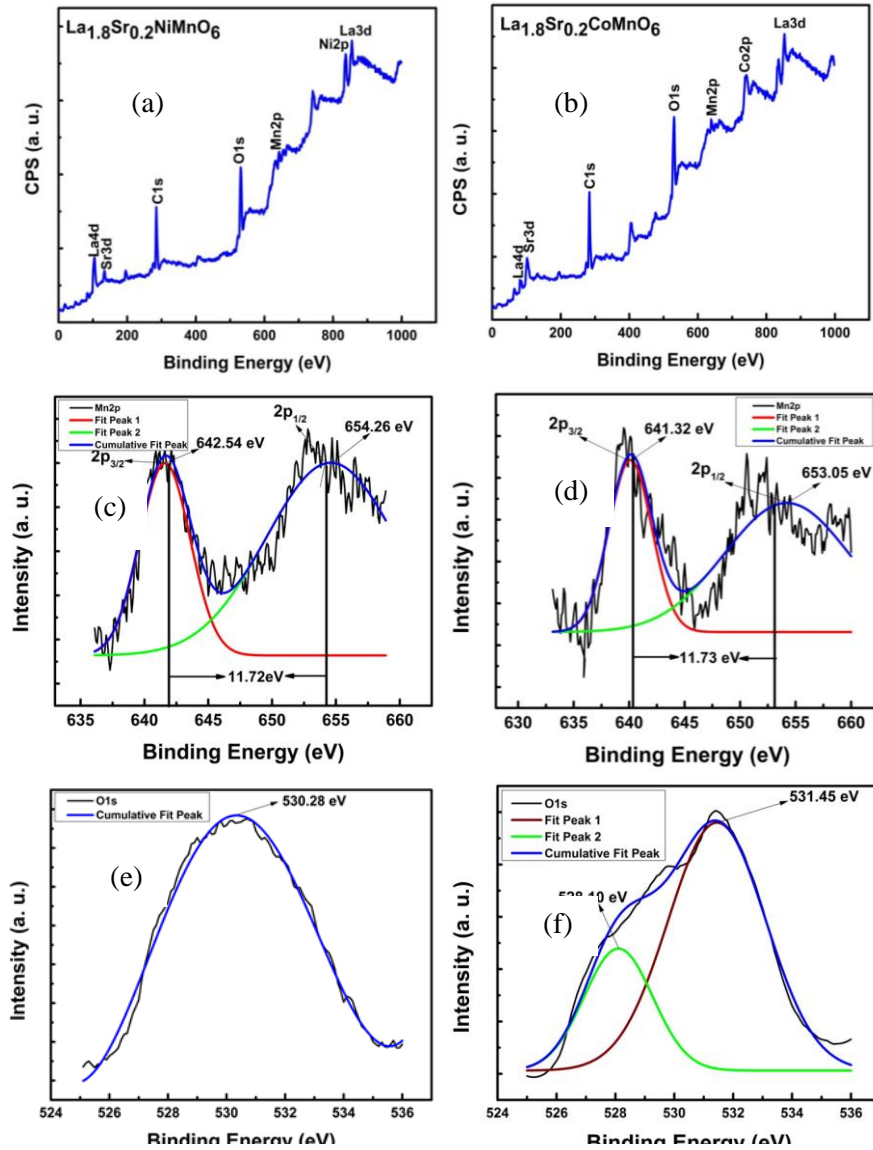


Figure 4. XPS spectra of all elements (a), (b); the Mn 2p (c), (d) and the O 1s (e), (f); of $\text{La}_{1.8}\text{Sr}_{0.2}\text{MMnO}_6$ (M = Ni, Co) manganites.

dependent ZFC and FC magnetization curves exhibit a sharp FM to PM transition at 280 K. [24, 27, 43-49] It has also been found that depending on the synthesis conditions, LNMO can exhibit one and more magnetic transitions. It is reported that LNMO shows two FM transitions occurring at $T_{c1} \sim 280$ K and $T_{c2} \sim 150$ K. [7, 28, 43, 44, 50]

However, in the present investigation, we have observed a sharp transition at 220 ± 2 K due to the substitution of Sr in LCMO manganites (Figures 5(c, d)). In the Figure 5(c), it is observed that there is a small dip in the plot around ~ 50 K that can be attributed to the presence of small amounts of hausmanite (Mn_3O_4), probably due to the presence of the higher electro positivity of Sr ions [51].

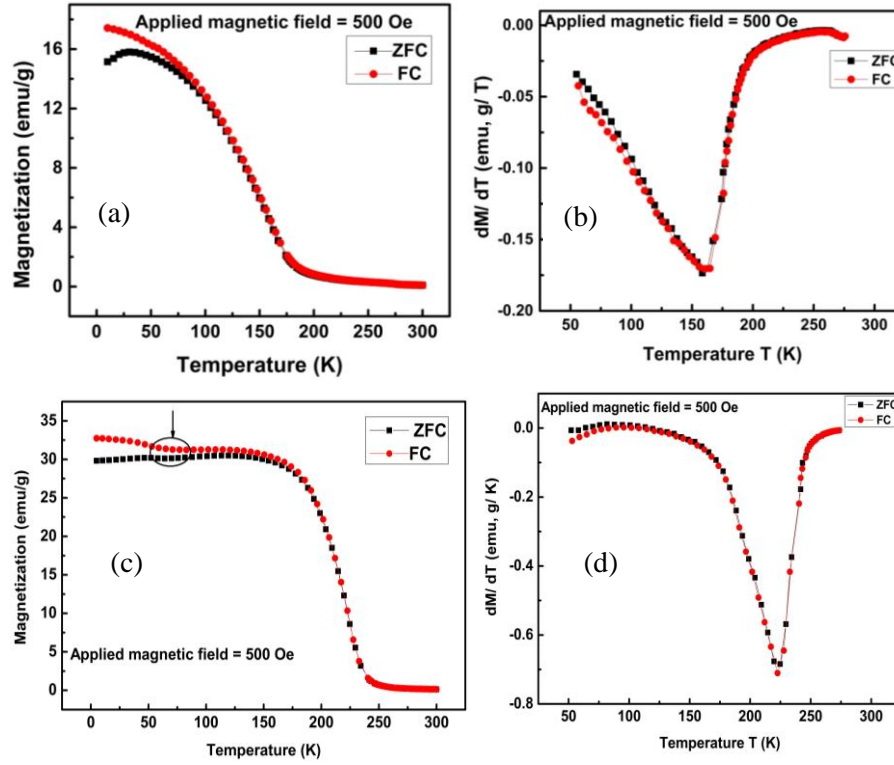


Figure 5. Temperature dependence of magnetization of $\text{La}_{1.8}\text{Sr}_{0.2}\text{MMnO}_6$ ($M = \text{Ni}, \text{Co}$) manganites Zero-Field-Cooled (ZFC) and Field-Cooled (FC) magnetization as a function of temperature (a) and (c). The first derivative of the temperature dependent magnetization (dM/dT) (b) and (d).

It is reported that the temperature dependence ZFC and FC magnetization curves exhibit a sharp FM to PM transition at 230 K for parent LCMO. [26] It has also been found that depending on the synthesis conditions LCMO can also exhibit one and more magnetic transitions. LCMO shows two FM transitions occurring at $T_{c1} \sim 220$ K and $T_{c2} \sim 150$ K. [52] Besides, other researchers reported that three distinct anomalies can be observed in both FC and ZFC curves of LCMO. The high-temperature anomaly is $T_{c1} \sim 210$ K, the medium-temperature anomaly locates at $T_{c2} \sim 150$ K, and the low-temperature anomaly is $T_{c3} \sim 80$ K. [30] The multiple magnetic phase transitions have been reported earlier for both $\text{La}_2\text{CoMnO}_6$ ceramics and thin films. [7, 26, 28, 51-57] In this case, due to the substitution of Sr a sharp transition was observed at 220 ± 2 K.

Notably, LNMO and LCMO can exhibit one or more magnetic transitions. In LNMO, an ordered sublattice with high spin Ni^{2+} and Mn^{4+} gives a FM transition at 280 K, while a disordered sublattice with low spin Ni^{3+} and high spin Mn^{3+} results in a FM transition below 150 K. [7, 28, 43, 44, 50] Similarly an ordered sublattice with high spin Co^{2+} and Mn^{4+} pairs in LCMO gives a FM transition at 220 K, while a disordered sublattice with low spin Co^{3+} and high spin Mn^{3+} results in a FM transition below 150 K. [52] The observed FM transition can be assigned to the superexchange interaction between $\text{M}^{2+}-\text{O}^{2-}-\text{Mn}^{4+}$ in La_2MMnO_6 ($M = \text{Ni}, \text{Co}$) manganites. However, the substitutions of La by Sr in LNMO and LCMO significantly affect the Curie temperature (T_c). The value of T_c for LSNMO and LSCMO is determined by the FM coupling intensity between Ni and Mn; and Co and Mn ions which might be associated with the influence

of modified structural parameters including the bond length and bond angle between M^{2+} - O^{2-} - Mn^{4+} .

It is evident that temperature dependent ZFC and FC magnetization curves of LSNMO exhibit a sharp FM to PM transition at 160 ± 2 K which is around 120 K less than that of parent LNMO. On the other hand, temperature dependence ZFC and FC cooled magnetization curves of LSCMO exhibit a sharp FM to PM transition at 220 ± 2 K which is around 8 K less than that of parent LCMO. The transition temperatures suggest that the effect of Sr on the transition temperature of LNMO is more significant than that in LCMO. Notably, microstructures obtained from FESEM images show that substitution of Sr in the $La_{1.8}Sr_{0.2}MMnO_6$ ($M = Ni, Co$) has demoted the grain growth process during sintering. We observed a correlation between the microstructural characteristics of LNMO and LCMO manganites and their magnetic transition temperatures. The temperature dependent magnetization measurements (Figure 5) demonstrated that the T_c value is lower for Sr substituted LSNMO manganite for which the average grain size is smaller compared to that of LSCMO.

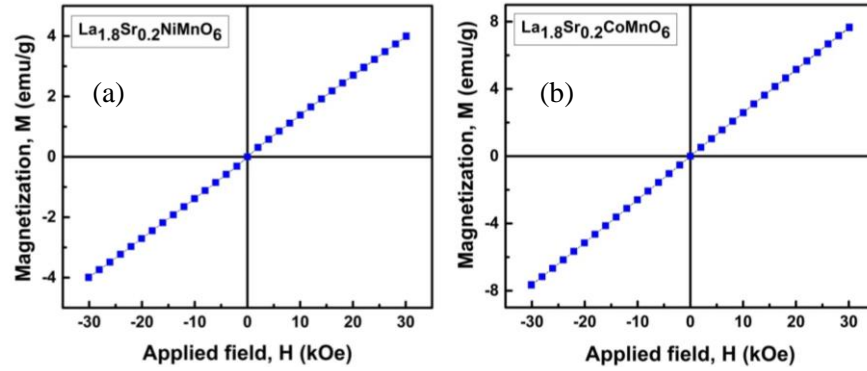


Figure 6. The room temperature M-H curves of $La_{1.8}Sr_{0.2}MMnO_6$ ($M = Ni, Co$) bulk materials.

The magnetization versus magnetic field (M-H) curves of $La_{1.8}Sr_{0.2}MMnO_6$ ($M = Ni, Co$) bulk materials were carried out at 300 K as represented in Figures 6(a, b). The unsaturated linear curves without any detectable hysteresis, clearly indicate the paramagnetic nature of the corresponding bulk sample.

Conclusions

The Sr substituted $La_{1.8}Sr_{0.2}MMnO_6$ ($M = Ni, Co$) manganites have been successfully synthesized and characterized. The average grain size of $La_{1.8}Sr_{0.2}NiMnO_6$ and $La_{1.8}Sr_{0.2}CoMnO_6$ have been found in the range 0.2~0.7 μm and 0.1~2.8 μm , respectively. The X-ray diffraction patterns revealed that Sr substituted $La_{1.8}Sr_{0.2}MMnO_6$ ($M = Ni$ and Co) manganites has a rhombohedral structure. The chemical binding energies of the constituent elements of Sr substituted LSNMO and LSCMO manganites were confirmed from XPS analysis. For Sr substituted LSNMO, the FM to PM transition is found at around 160 ± 2 K whilst for LSCMO, the transition is observed at around 220 ± 2 K. The value of the transition temperature is lower for Sr substituted LSNMO manganite for which the average grain size is smaller compared to that of LSCMO. We may conclude that the addition of Sr in $La_{1.8}Sr_{0.2}MMnO_6$ manganites produced considerable modifications in the

morphological, structural and magnetic properties of these manganites which might be useful in technological applications.

Acknowledgments

This work was supported by The Ministry of Science and Technology, Government of Bangladesh under research Grant No.: 39.009.002.01.00.053.2014-2015/PHY'S-273/ (26.01.2015). The magnetization measurements using SQUID were conducted in the Institute for Molecular Science (IMS), supported by Nanotechnology Platform Program (Molecule and Material Synthesis) of the Ministry of Education, Culture, Sports, Science and Technology (MEXT), Japan.

References:

- [1] Singh MP, Truong K, Fournier P. Magnetodielectric effect in double perovskite $\text{La}_2\text{CoMnO}_6$ thin films. *Appl Phys Lett*. 2007;91:042504.
- [2] Singh MP, Carpentier S, Truong K, Fournier P. Evidence of bi-domain structure in double-perovskite $\text{La}_2\text{CoMnO}_6$ thin films. *Appl Phys Lett*. 2007;90:211915.
- [3] Lin YQ, Chen XM. Dielectric, ferromagnetic characteristics, and room-temperature magnetodielectric effects in double perovskite $\text{La}_2\text{CoMnO}_6$ ceramics. *J Am Ceram Soc*. 2011;94:782-787.
- [4] Singh MP, Truong KD, Jandl S, Founier P. Multiferroic double perovskites: opportunities, issues, and challenges. *J Appl Phys*. 2010;107:09D917.
- [5] Zhu M, Lin Y, Edward WCL, Wang Q, Zhao Z, Xie W. Electronic and magnetic properties of $\text{La}_2\text{NiMnO}_6$ and $\text{La}_2\text{CoMnO}_6$ with cationic ordering. *Appl Phys Lett*. 2010;100:062406.
- [6] Mandal TK, Felser C, Greenblatt M, Kubler J. Magnetic and electronic properties of double perovskites and estimation of their curie temperatures by ab initio calculations. *Phys Rev B*. 2008;78:134431.
- [7] Dass RI, Goodenough JB. Multiple magnetic phases of $\text{La}_2\text{CoMnO}_6$. *Phys Rev B*. 2003;67:014401.
- [8] Yáñez-Vilar S, Mun ED, Zapf VS, Ueland BG, Gardner JS, Thompson JD, Singleton J, Sánchez-Andújar M, Mira J, Biskup N, Señarís-Rodríguez MA, Batista CD. Multiferroic behavior in the double-perovskite $\text{Lu}_2\text{MnCoO}_6$. *Phys Rev B*. 2011;84:134427.
- [9] Jeroen van den B, Daniel IK. Multiferroicity due to charge ordering. *J Phys Condens Matter*. 2008;20:434217.
- [10] Burnus T, Hu Z, Hsieh HH, Joly VLJ, Joy PA, Haverkort MW, Wu H, Tanaka A, Lin HJ, Chen CT, Tjeng LH. Local electronic structure and magnetic properties of $\text{aMn}_{0.5}\text{Co}_{0.5}\text{O}_3$ studied by X-ray absorption and magnetic circular dichroism spectroscopy. *Phys Rev B*. 2010;77(12):125124.
- [11] Mahato RN, Sethupathi K, Sankaranarayanan V. Intrinsic dielectric properties of magnetodielectric $\text{La}_2\text{CoMnO}_6$. *J Appl Phys*. 2010;107(9):09D714.
- [12] Padhan P, Guo HZ, LeClair P, Gupta A. Dielectric relaxation and magnetodielectric response in epitaxial thin films of $\text{La}_2\text{NiMnO}_6$. *Appl Phys Lett*. 2008;92(2):022909.
- [13] Choudhury D, Mandal P, Mathieu R, Hazarika A, Rajan S, Sundaresan A, Waghmare UV, Knut R, Karis O, Nordblad P, Sarma DD. Near-Room-Temperature colossal magnetodielectricity and multiglass properties in partially disordered $\text{La}_2\text{NiMnO}_6$. *Phys Rev Lett*. 2012;108:127201.

- [14] Das H, Waghmare UV, Saha-Dasgupta T, Sarma DD. Electronic structure, phonons, and dielectric anomaly in ferromagnetic insulating double perovskite $\text{La}_2\text{NiMnO}_6$. *Phys Rev Lett*. 2008;100:186402.
- [15] Katsura H, Nagaosa N, Balatsky AV. Spin current and magnetoelectric effect in noncollinear magnets. *Phys Rev Lett*. 2005;95:057205.
- [16] Lawes G, Ramirez AP, Varma CM, Subramanian MA. Magnetodielectric effects from spin fluctuations in isostructural ferromagnetic and antiferromagnetic systems. *Phys Rev Lett*. 2003;91:257208.
- [17] Tokura Y, Seki S. Multiferroics with spiral spin orders. *Adv Mater*. 2010;22(14):1554.
- [18] Solovyev I, Hamada N, Terakura K. Crucial role of the lattice distortion in the magnetism of LaMnO_3 . *Phys Rev Lett*. 1996;76:4825.
- [19] Senaris-Rodriguez MA, Goodenough JB. LaCoO_3 revisited. *J Solid State Chem*. 1995;116:224.
- [20] Zener C. Interaction between the shells in the transition metals. *Phys Rev*. 1951;81:440.
- [21] De-Gennes PG. Effects of double exchange in magnetic crystals. *Phys Rev*. 1960;118:141.
- [22] Basith MA, Manjura Hoque Sk, Shahparan Md, Hakim MA, Huq M. Temperature features of magnetoresistance of layered manganites $\text{La}_2\text{Sm}_{0.4}\text{Sr}_{0.6}\text{Mn}_2\text{O}_7$. *Physica B*. 2007;395:126-129.
- [23] Basith MA, Khan FA, Ahammad B, Kubota S, Hirose F, Ngo DT, Tran QH, Mølhave K. Tunable exchange bias effect in magnetic $\text{Bi}_{0.9}\text{Gd}_{0.1}\text{Fe}_{0.9}\text{Ti}_{0.1}\text{O}_3$ nanoparticles at temperatures up to 250 K. *J App Phys*. 2015;118:023901.
- [24] Yuqiao G, Lei S, Shiming Z, Jiyin Z, Cailin W, Wenjie L, Shiqiang W. Tunable exchange bias effect in Sr-doped double perovskite $\text{La}_2\text{NiMnO}_6$. *J Phys D:Appl Phys*. 2013;46(6):175302.
- [25] Wenjie L, Lei S, Shiming Z, Jiyin Z, Yang L, Yuqiao G. Size-Dependent multiple magnetic phases and exchange bias effect in hole-doped double perovskite $\text{La}_{1.6}\text{Sr}_{0.4}\text{NiMnO}_6$. *J Phys D:Appl Phys*. 2014;47(8):485003.
- [26] Krishna Murthy J, Devi Chandrasekhar K, Murugavel S, Venimadhava A. Investigation of the intrinsic magneto dielectric effect in $\text{La}_2\text{CoMnO}_6$: role of magnetic disorder. *J Mater Chem C*. 2015;3:836–843.
- [27] Guo Y, Shi L, Zhou S, Zhao J, Liu W. Near room-temperature magneto resistance effect in double perovskite $\text{La}_2\text{NiMnO}_6$. *Appl Phys Letts*. 2013;102:222401.
- [28] Bull CL, Gleeson D, Knight KS. Determination of B-site ordering and structural transformations in the mixed transition metal perovskites $\text{La}_2\text{CoMnO}_6$ and $\text{La}_2\text{NiMnO}_6$. *J Phys:Condens Matter*. 2003;15:4927.
- [29] Al-Haj M. X-ray diffraction and magnetization studies of BiFeO_3 multiferroic compounds substituted by Sm^{3+} , Gd^{3+} , Ca^{2+} . *Cryst Res Technol*. 2010;45:89-93.
- [30] Goodenough JB, Wold A, Arnott RJ, Menyuk N. Relationship between crystal symmetry and magnetic properties of ionic compounds containing Mn^{++} . *Phys Rev*. 1961;124:373.
- [31] Balli M, Fournier P, Jandl S, Truong KD, Gospodinov MM. Analysis of the phase transition and magneto-thermal properties in $\text{La}_2\text{CoMnO}_6$ single crystals. *J Appl Phys*. 2014;116:073907.
- [32] Pal P, Giri AK, Mahanty S, Panda AB. Morphology-mediated tailoring of the performance of porous nanostructured Mn_2O_3 as an anode material. *Cryst Eng Comm*. 2014;16:10560.

- [33] Han SW, Lee JD, Kim KH, Song H, Kim WJ, Kwon SJ, Lee HG, Hwang C, Jeong JI, Kang JS. Electronic structures of the CMR perovskites $R_{1-x}A_x\text{MnO}_3$ ($R = \text{La, Pr}$; $A = \text{Ca, Sr, Ce}$) using photoelectron spectroscopy. *J Korean Phys Soc.* 2002;40(3):501-510.
- [34] Fang LA, Liu JA, Ju S, Zheng FG, Dong W, Shen MR. Experimental and theoretical evidence of enhanced ferromagnetism in sonochemical synthesized BiFeO_3 nanoparticles. *Appl Phys Lett.* 2010;97:242501.
- [35] Das R, Sarkar T, Mandal K. Multiferroic properties of Ba^{2+} and Gd^{3+} co-doped bismuth ferrite: magnetic, ferroelectric and impedance spectroscopic analysis. *J Phys D:Appl Phys.* 2012;45:45500212.
- [36] Beyreuther E, Grafström S, Eng LM, Thiele C and Dörr K. XPS investigation of Mn valence in lanthanum manganite thin films under variation of oxygen content. *Phys Rev B.* 2006;73:155425.
- [37] Liang JJ, Weng HS. Catalytic properties of lanthanum strontium transition metal oxides ($\text{La}_{1-x}\text{Sr}_x\text{BO}_3$; $B = \text{manganese, iron, cobalt, nickel}$) for toluene oxidation. *Ind Eng Chem Res.* 1993;32:2563.
- [38] Decorse P, Quenneville E, Poulin S, Meunier M, Yelon A, Morin F. Chemical and structural characterization of $\text{La}_{0.5}\text{Sr}_{0.5}\text{MnO}_3$ thin films prepared by Pulsed-laser deposition. *J Vac Sci Technol A.* 2001;19:910.
- [39] Choi J, Dulli H, Liou SH, Dowben PA, Langell MA. The influence of surface terminal layer and surface defects on the electronic structure of CMR perovskites: $\text{La}_{0.65}\text{A}_{0.35}\text{MnO}_3$ ($A = \text{Ca, Sr, Ba}$). *Phys Status Solidi B.* 1999;45:214.
- [40] Choi J, Zhang J, Liou SH, Dowben PA, Plummer EW. The surfaces of the perovskite manganites $\text{La}_{1-x}\text{Ca}_x\text{MnO}_3$. *Phys Rev B.* 1999;59:13453.
- [41] Zhang-Steenwinkel Y, Beckers J, Blik A, Surface properties and catalytic performance in CO oxidation of cerium substituted Lanthanum–Manganese Oxides. *Appl Catal A.* 2002;79:235.
- [42] Ponce S, Pena MA, Fierro JLG. Surface properties and catalytic performance in methane combustion of Sr-substituted lanthanum manganites. *Appl Catal B.* 2000;24:193-205.
- [43] Goodenough JB. *Magnetism and the Chemical Bond.* Inter Science Publ NY. 1976.
- [44] Dass RI, Yan JQ, Goodenough JB. Oxygen stoichiometry, ferromagnetism and Transport properties of $\text{La}_{2-x}\text{NiMnO}_{6+\delta}$. *Phys Rev B.* 2003;68:064415.
- [45] Zhou S, Shi L, Yang H, Zhao J. Evidence of short-range magnetic ordering above T_C in the double perovskite $\text{La}_2\text{NiMnO}_6$. *Appl Phys Lett.* 2007;91:172505.
- [46] Rogado NS, Li J, Sleight AW, Subramanian MA. Magnetocapacitance and magnetoresistance near room temperature in a ferromagnetic semiconductor: $\text{La}_2\text{NiMnO}_6$. *Adv. Mater.* 2005;17:2225.
- [47] Hashisaka M, Kan D, Masuno A, Takano M, Shimakawa Y, Terashima T, Mibu K. Epitaxial growth of ferromagnetic $\text{La}_2\text{NiMnO}_6$ with ordered double-perovskite structure. *Appl Phys Lett.* 2006;89:032504.
- [48] Wang XJ, Sui Y, Li Y, Li L, Zhang XQ, Wang Y, Liu ZG, Su WH, Tang JK. The Influence of the antiferromagnetic boundary on the magnetic property of $\text{La}_2\text{NiMnO}_6$. *Appl Phys Lett.* 2009;95:252502.
- [49] Zhou SM, Guo YQ, Zhao JY, Zhao SY, Shi L. Nature of short-range ferromagnetic ordered state above T_C in double perovskite $\text{La}_2\text{NiMnO}_6$. *Appl Phys Lett.* 2010;96:262507.

- [50] Singh MP, Grygiel C, Sheets WC, Boullay P, Hervieu M, Prellier W, Mercey B, Simon C, Raveau B. Absence of long-range Ni/Mn ordering in ferromagnetic $\text{La}_2\text{NiMnO}_6$ thin films. *Appl Phys Lett*. 2007;91:012503.
- [51] Ahmad T, Ramanujachary KV, Lofland SE, Ganguli AK. Reverse micellar synthesis and properties of nanocrystalline GMR materials (LaMnO_3 , $\text{La}_{0.67}\text{Sr}_{0.33}\text{MnO}_3$ and $\text{La}_{0.67}\text{Ca}_{0.33}\text{MnO}_3$): ramifications of size considerations. *J Chem Sci*. 2006;118(6):513–518.
- [52] Joseph Joly VL, Khollam YB, Joy PA, Gopinath CS, Date SK. Unusual charge disproportionation and associated magnetic behaviour in nanocrystalline $\text{LaMn}_{0.5}\text{Co}_{0.5}\text{O}_3$. *Mater Lett*. 2000;46:261.
- [53] Lin YQ, Chen XM, Liu XQ. Dielectric, ferromagnetic characteristics and room temperature magnetodielectric effects in double perovskite $\text{La}_2\text{CoMnO}_6$ ceramics. *J Am Ceram Soc*. 2011;94(3):782–787.
- [54] Truong KD, Laverdière J, Singh MP, Jandl S, Fournier P. Impact of Co/Mn cation ordering on phonon anomalies in $\text{La}_2\text{CoMnO}_6$ double perovskites: raman spectroscopy. *Phys Rev B*. 2007;76(13):132413.
- [55] Guo HZ, Gupta A, Zhang J, Varela M, Pennycook SJ. Effect of oxygen concentration on the magnetic properties of $\text{La}_2\text{CoMnO}_6$ thin films. *Appl Phys Lett*. 2007;91(20):202509.
- [56] Guo HZ, Gupta A, Calvarese TG, Subramanian MA. Structural and magnetic properties of epitaxial thin films of the ordered double perovskite $\text{La}_2\text{CoMnO}_6$. *Appl Phys Lett*. 2006;89(26):262503.
- [57] Joy PA, Khollam YB, Date SK. Spin states of Mn and Co in $\text{LaMn}_{0.5}\text{Co}_{0.5}\text{O}_3$. *Phys Rev B*. 2000;62:8608.